

Voltammetric study of lead electrodeposition in the presence of sorbitol and morphological characterization

I.A. Carlos^{*}, J.L.P. Siqueira, G.A. Finazzi, M.R.H. de Almeida

Departamento de Química, Universidade Federal de São Carlos, C. P. 676, 13565-905 São Carlos, SP, Brazil

Received 20 December 2002; accepted 31 December 2002

Abstract

The potentiodynamic electrodeposition of lead on a 1010 steel substrate from a new electrolytic solution was studied in order to establish whether sorbitol additive is suitable for the production of lead film for use in lead batteries and whether this polyalcohol can be used in lead scrap recycling. It was observed that the presence of sorbitol in the plating bath proved to be critical, since in its absence it was impossible to prepare solutions of plumbite in NaOH <2.0 M, because PbO is insoluble. Under potentiodynamic conditions the lead deposits obtained on 1010 steel could be transformed into high purity lead powder by undercutting of the lead film during the anodic dissolution scan. With the help of scanning electron microscopy (SEM) photographs it was concluded that sorbitol reduced the lead dendritic growth more significantly than glycerol additive and that this new electrolytic solution could be used to recycle lead scrap.

© 2003 Elsevier Science B.V. All rights reserved.

Keywords: Lead deposits; Sorbitol; Recycling; 1010 steel

1. Introduction

Electrodeposition of lead [1–4] has been accomplished from various acid solutions: nitrate, fluoroborate, fluorosilicate, perchlorate, pyrophosphate, acetate, etc. As most acid electrolytes are toxic, alkaline electrolytes are more appropriate from an environmental standpoint. Moreover, new alkaline solutions have been developed to carry out lead plating and lead scrap recycling [5–9]. Alkaline electrolytes are valuable not only from the point of view of environmental protection but also for their low corrosiveness compared to acid electrolytes. We have been interested in the electrodeposition of lead onto AISI 1010 steel from alkaline solutions since we observed that the presence of additives in the plating bath has a beneficial effect on Pb and Cu/Sn electrodeposits [9,10]. These studies established that the additives tartrate, in the Cu/Sn, and glycerol in the Pb plating baths reduce strain and inhibit dendritic growth, respectively. Also, Molenaar and de Bakker [11] investigated the electrochemical process of tin electrodeposition and demonstrated that it is possible to avoid the spontaneous growth of tin crystals in the alkaline solution by the addition of sorbitol stabilizing agent.

In this context and continuing former studies, in this paper we review the production of lead films in an alkaline sorbitol bath, with particular emphasis on the optimization of the new electrolytic solution for use in lead battery technology and lead scrap recycling.

2. Experimental

All chemicals were analytical grade. Double-distilled water was used throughout. Each electrochemical experiment was performed in a bath containing 0.1 M Pb(NO₃)₂ + NaOH at various concentrations (0.40, 0.60, 0.8, 1.0, 2.0 and 3.0 M), in the presence and absence of 0.2 M sorbitol. After approximately 6 months, the bath containing 0.40 M NaOH became unstable, with formation of a yellow powder, probably lead oxide, and so proved unsuitable.

A 1010 steel disk (0.5 cm²), a Pt plate and a Hg/HgO/1 M NaOH electrode with an appropriate Luggin capillary were employed as working, auxiliary and reference electrodes, respectively. The 1010 steel disk (AISI), from CSN Co., contained 0.044% P, 0.08% C, 0.3% Mn and 0.05% S. Immediately prior to the electrochemical measurements the 1010 steel alloy working electrodes were abraded with emery paper, then rinsed with double-distilled water. Potentiodynamic curves were recorded using a PAR model 366

^{*} Corresponding author. Tel.: +55-16-260-8208; fax: +55-16-260-8350.
E-mail address: ivani@dq.ufscar.br (I.A. Carlos).

potentiostat/galvanostat and a plotting recorder. Electrochemical efficiency (ϕ_e) was calculated from the ratio of dissolution to deposition charges. All experiments were carried out at room temperature (25 °C). Scanning electron microscopy (SEM) micrographs were taken with Carl Zeiss, Model DMS 940A and Phillips, Model XL 30 FEG electron microscopes.

3. Results and discussion

3.1. Electrodeposition of Pb on 1010 steel in the presence of sorbitol

Fig. 1a shows voltammograms for the stationary 1010 steel substrate in the 0.1 M Pb^{2+} plating bath at various NaOH concentrations: 0.6, 0.8, 1.0 and 2.0 M, all in the presence of 0.2 M sorbitol. The main feature of these voltammograms is the cathodic peak, characterized by a steep increase in current density, after which the current density decreases, owing to mass-transport limitation. Still in Fig. 1a, the increase in the current density towards a further cathodic peak may be associated with hydrogen evolution and/or an increase in the area of deposit, suggesting a second nucleation process. Also, it can be observed that the lead-plating rate is affected kinetically by hydroxide ion only at 2.0 M NaOH, when the current density magnitudes

increase significantly. Nevertheless, hydroxide ion does not affect the plating thermodynamically, since the initial deposition potential does not change to more cathodic values with increasing NaOH concentration. Fig. 1b (with no Pb nitrate) shows that H_2 evolution does not affect the voltammetric deposition of Pb in the initial moments of the process. It is only really significant at potentials beyond -1.2 V. Also, it was observed that during the dissolution of the lead film (anodic portion of Fig. 1c) undercutting of the deposit occurred at the top of the anodic peak.

It can be inferred from these results that the presence of sorbitol in the plating bath proved to be very useful, since in its absence it was impossible to prepare solutions of plumbite in NaOH < 2.0 M, since PbO is insoluble. Thus, the plating bath containing 0.1 M Pb^{2+} , 2.0 M NaOH and 0.2 M sorbitol was chosen for the subsequent studies of the deposition process, since this solution is more conductive and leads to higher rates than the baths with lower NaOH concentrations.

By comparing the effects of the additives sorbitol (solid line) and glycerol (dotted line) and the absence of these additives (dashed line) in the plating bath, Fig. 2, it can be seen that the presence of sorbitol in the bath shifts the lead deposition potential to more cathodic values and reduces significantly the deposition current density in the region of the cathodic peak. The reduction of the deposition current density may represent an inhibition of the deposition in the

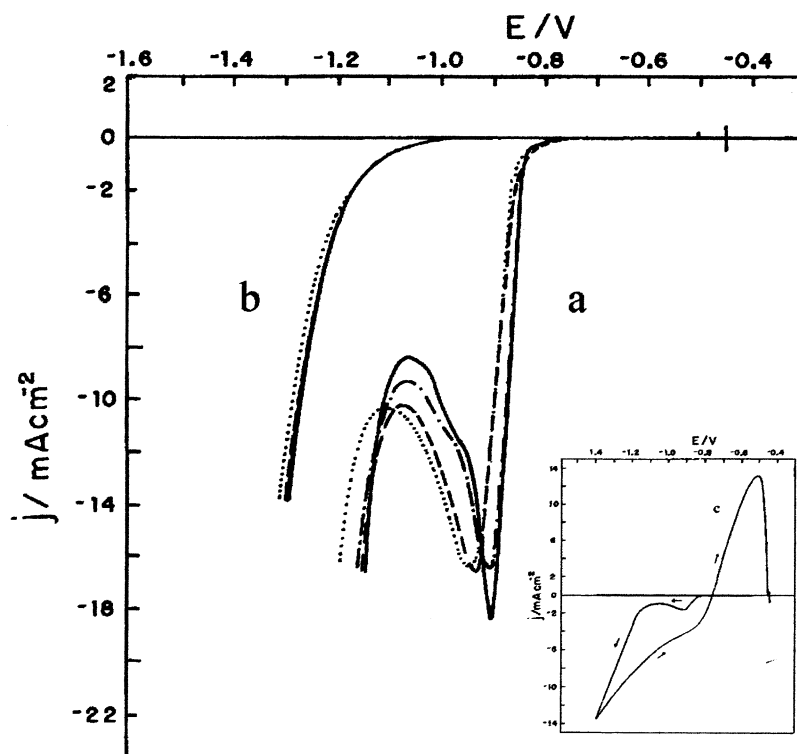


Fig. 1. Voltammetric curves for 1010 steel substrate in: (a) 0.1 M $\text{Pb}(\text{NO}_3)_2$ + 0.6 (\cdots), 0.8 ($-\cdot-\cdot-$), 1.0 ($-\cdot-\cdot-$), 2.0 ($—$) M NaOH, all in the presence of 0.2 M sorbitol; (b) 0.6 (\cdots), 0.8 ($-\cdot-\cdot-$), 1.0 ($-\cdot-\cdot-$), 2.0 ($—$) M NaOH, all in the presence of 0.2 M sorbitol; (c) 0.1 M $\text{Pb}(\text{NO}_3)_2$ + 2.0 M NaOH + 0.2 M sorbitol; at 10 mV s^{-1} . Potential, in V, vs. $\text{Hg}/\text{HgO}/1 \text{ M NaOH}$.

region of cathodic peak, or a modification in the morphology of the deposit. The latter effect has been observed during lead [9] and copper electrodeposition [12] from an alkaline glycerol plating bath and also copper plating in the presence of sorbitol [13], when inhibition of crystallite growth took place. This fall in current density is more significant in the presence of added sorbitol ($\sim 17 \text{ mA cm}^{-2}$, Fig. 2, solid line) than in the presence of glycerol ($\sim 24 \text{ mA cm}^{-2}$, Fig. 2, dotted line).

These results are significant since the presence of sorbitol in the deposition bath may lead to a better quality deposit than in the presence of glycerol.

Fig. 3 illustrates the effect of increasing the deposition charge densities (q_d) on the current efficiency (ϕ_e) of the lead deposition process. The lead films were obtained potentiodynamically, from -0.450 V to various E_d , at different charge densities (q_d). It can be seen that increasing the q_d increases the ϕ_e values and that they are significantly lower than 100%, probably due to the low nucleation rate when the deposition potential (E_d) is less cathodic than -0.86 V and undercutting of lead film for E_d more cathodic than -1.0 V . Also, the ϕ_e values in the presence of glycerol [9] ($\sim 70\%$) were higher than in the presence of sorbitol ($\sim 35\%$) for deposition potentials less cathodic than -1.4 V . These results corroborate the lower current densities obtained in the presence of sorbitol than in the presence of glycerol (Fig. 2), suggesting that sorbitate anion inhibits the nucleation and growth rates. However, for deposition potentials more cathodic than -1.0 V , in the presence of glycerol or sorbitol, the ϕ_e values are the same ($\sim 40\%$), due

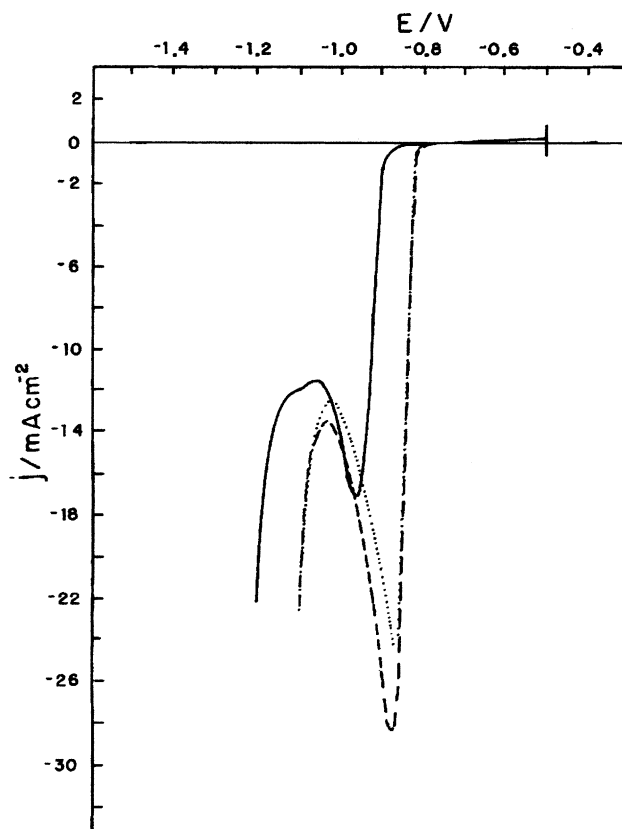


Fig. 2. Voltammetric curves (vs. Hg/HgO/1 M NaOH) for 1010 steel substrate in: (a) 0.1 M $\text{Pb}(\text{NO}_3)_2$ + 2.0 M NaOH (dashed line), (b) 0.1 M $\text{Pb}(\text{NO}_3)_2$ + 2.0 M NaOH + 0.2 M sorbitol (solid line), (c) 0.1 M $\text{Pb}(\text{NO}_3)_2$ + 2.0 M NaOH + 0.2 M glycerol (dotted line); at 10 mV s^{-1} .

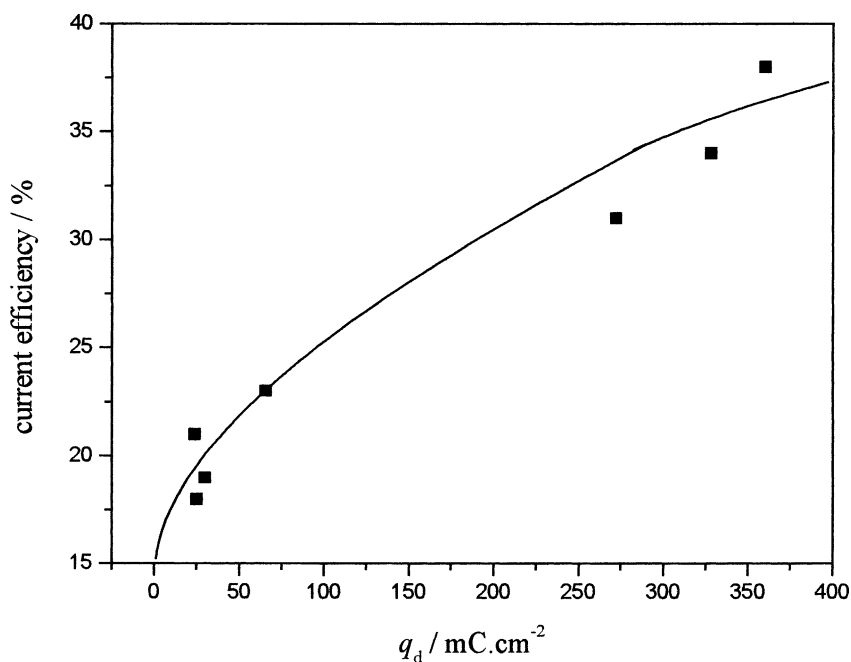


Fig. 3. Electrochemical efficiency (ϕ_e) of lead electrodeposits obtained at different deposition charges from 0.1 M $\text{Pb}(\text{NO}_3)_2$ + 2.0 M NaOH + 0.2 M sorbitol.

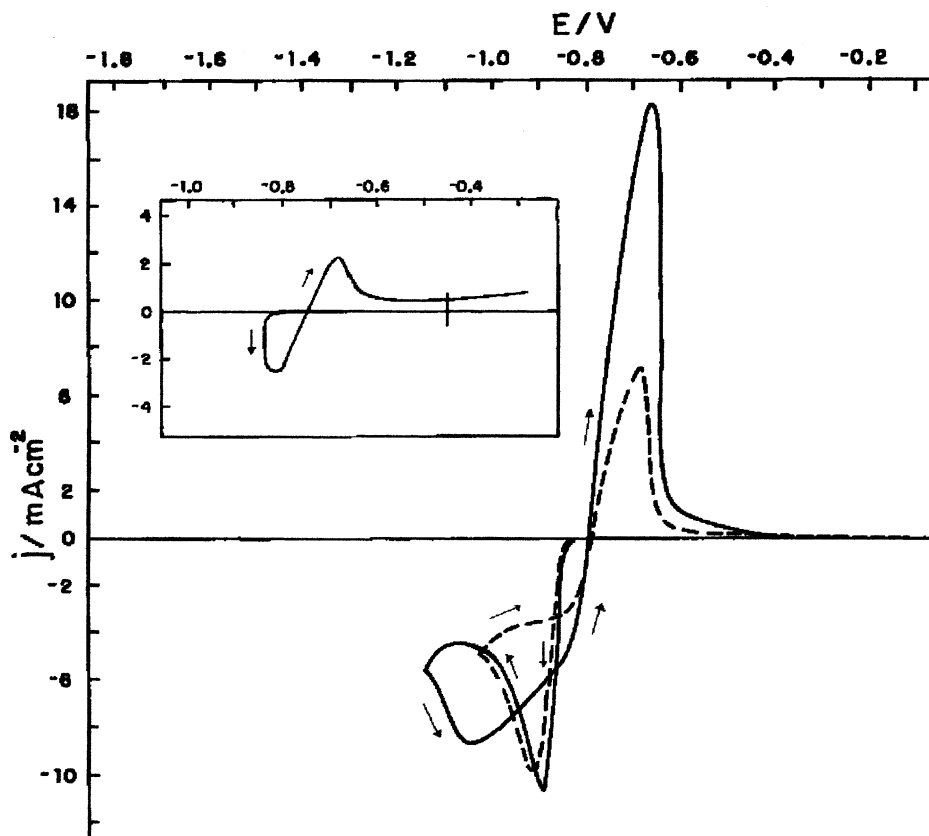


Fig. 4. Voltammetric curves (vs. Hg/HgO/1 M NaOH) for 1010 steel substrates in 0.1 M $\text{Pb}(\text{NO}_3)_2$ + 2.0 M NaOH + 0.2 M sorbitol—effect of the cathodic potential limit values: -0.86 V (inset), -1.0 V (dashed line) and -1.1 V (solid line); at 10 mV s^{-1} .

to the deposit undercutting that occurs at the top of the anodic peak during the dissolution of lead films.

To characterize the cathodic process occurring in the presence of sorbitol bath better, the sweep was reversed at various potentials (Fig. 4). When the sweep was reversed at -0.86 V (inset in Fig. 4), an increase in cathodic current and a nucleation loop were observed, suggesting that the metal deposition occurred by nucleation [14]. After the nucleation loop, the cathodic current decreased quickly before the formation of an anodic peak. When the sweep was reversed at -1.0 V (dashed line), the current decreased, indicating that the plating process was under diffusion control [15,16]. Finally, reversing the sweep at -1.1 V (solid line), the current increased as in the first case (inset in Fig. 4) indicating a second process of nucleation and growth. Also, it can be seen that in the presence of sorbitol there exists a lead nucleation overpotential (~ 80 mV), which was not observed in its absence [9], but is comparable to that in the presence of glycerol in the plating bath (~ 90 mV) [9]. It can be inferred from these results that sorbitol and glycerol anions hinder the deposition process thermodynamically.

Fig. 5a shows a set of voltammograms obtained at various sweep rates from a bath containing 0.1 M Pb^{2+} , 2.0 M NaOH and 0.2 M sorbitol. The current density at the

cathodic peak exhibits a steep increase with the sweep rate. This is because the higher the scanning rate, the lower the fall in concentration of Pb^{2+} species at the metal/solution interface, and this leads to higher current densities. It can be inferred from these curves that the rate of lead deposition is controlled by mass transport in the regions beyond the cathodic peak. Fig. 5b shows that peak current density (j_p) increases with $v^{1/2}$, but is not proportional. This result suggests that the lead electrodeposition process is quasi-reversible in this region [15,16]. Fig. 5c shows that the peak potential (E_p) shifts negatively with increasing v , confirming the results of Fig. 5b.

To verify the observations made with the stationary electrode concerning the control of the deposition process by mass transport, experiments were done with a rotating disk electrode (RDE). Fig. 6 displays voltammetric curves with the RDE at various speeds of rotation, and it is clear that from the start of the deposition there is a contribution from mass transport control, as the deposition current densities are dependent on the speed of rotation, and that beyond the cathodic peak mass transport becomes important. Also, the current densities on the rotating disk electrode are much higher than on the stationary, indicating that the current densities observed on the stationary electrode are limited by mass transport. The diffusion coefficient

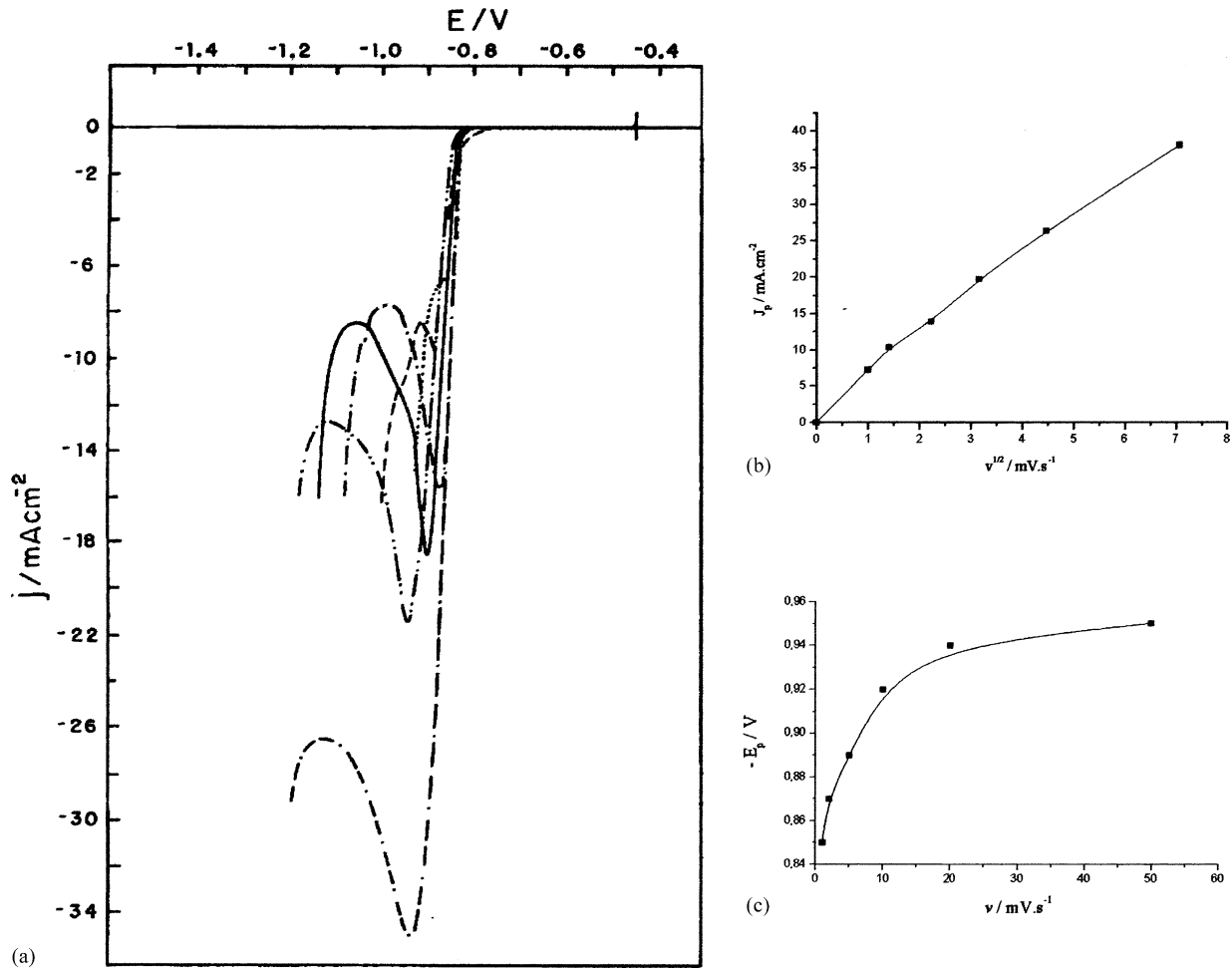


Fig. 5. Voltammetric curves (vs. Hg/HgO/1 M NaOH) for 1010 steel substrates in: (a) 0.1 M $\text{Pb}(\text{NO}_3)_2$ + 2.0 M NaOH + 0.2 M sorbitol at various sweep rates ($\text{v}/\text{mV s}^{-1}$): (\cdots) 1.0; ($-$) 2.0; ($- -$) 5.0; ($—$) 10; ($- \cdot - \cdot$) 20; ($- - - -$) 50; (b) variation of j_p with $v^{1/2}$ and (c) variation of E_p with v , for lead electrodeposition on steel substrate.

(D_0) of the lead complex was obtained from the RDE studies. Assuming a kinematic viscosity of $0.01 \text{ cm}^2 \text{ s}^{-1}$, and a roughness factor of ~ 2 (AISI 1010 steel substrate), the value of the coefficient of diffusion was $4.0 \times 10^{-6} \text{ cm}^2 \text{ s}^{-1}$. This value, as expected, is smaller than the D_0 of lead sulphate, $9.8 \times 10^{-6} \text{ cm}^2 \text{ s}^{-1}$ [17], at 25°C .

Finally, it can be concluded from the potentiodynamic curves for the 1010 steel electrode in the Pb plating baths, in the presence of sorbitol, that initial deposition rates are high, but lower than in either the absence or presence of glycerol (Fig. 2). Thus, the growth rate of the crystallites is relatively more significant than the nucleation rate, although both are slower than in the presence of glycerol in the plating bath; as a consequence, the deposits are less dendritic.

3.2. Scanning electronic microscopy

Figs. 7–9 show the physical appearance under SEM of electrodeposited lead films obtained with sorbitol present in the plating bath. When the potential was swept from -0.45

to -0.86 V (Fig. 1, solid line), the substrate was totally covered in coalesced lead crystallites (Fig. 7a and b).

In the potential range from -0.45 to -1.05 V (Fig. 1, solid line) lead globular crystallites and dendrites dispersed could be observed (Fig. 8a and b).

After the potential scan from -0.45 to -1.15 V (Fig. 1, solid line), gave an initial layer of coalesced lead crystallites, which was seen totally covering the substrate, and over these many dendrites and clusters were scattered (Fig. 9a and b). These results corroborate the increase in current density beyond -1.15 V observed in Fig. 4 (solid line) and confirm the second nucleation process.

It may be inferred from these results that the best condition in which to obtain the lead film is at a deposition potential of -0.86 V , because the dendrites are absent. Also, the sorbitate anion gives rise to smaller dendrites of lead, at or beyond the deposition potential of around -1.05 V than the glycerinate anion [9]. Thus, it may be concluded that the sorbitol works better than glycerol as a growth inhibitor, refining the lead deposit.

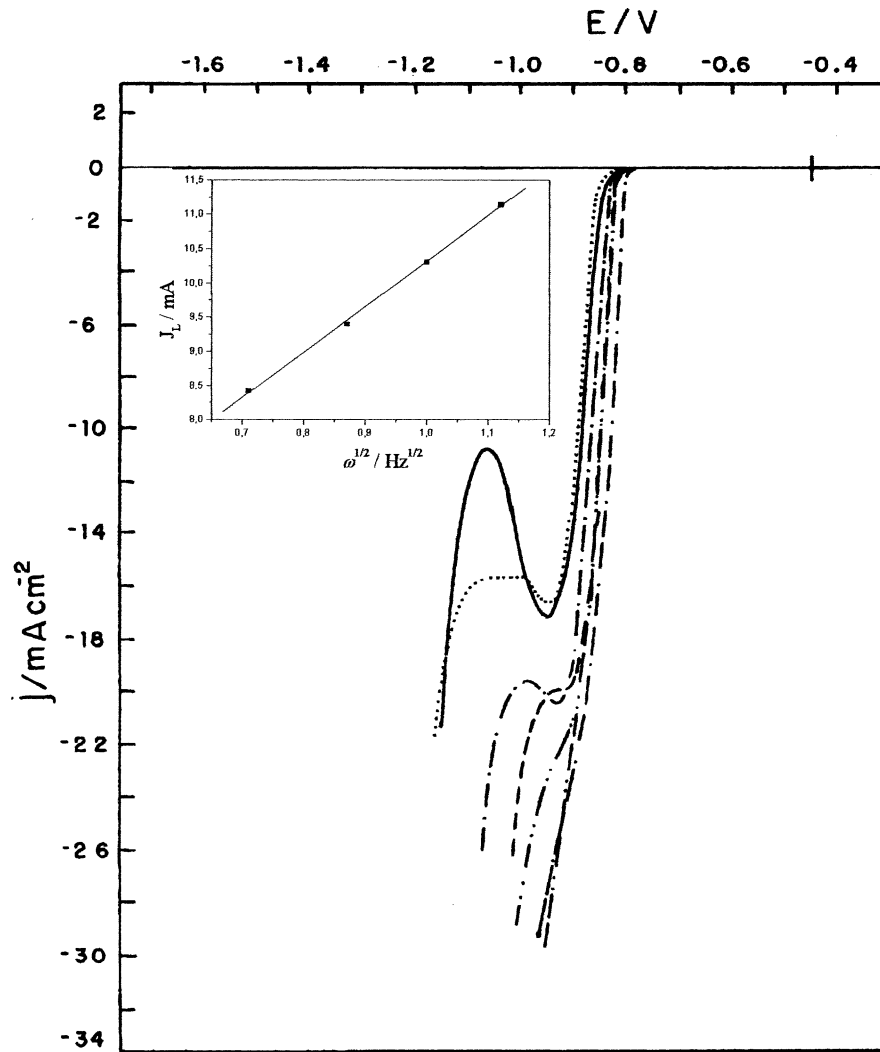


Fig. 6. Voltammetric curves (vs. Hg/HgO/1 M NaOH) for 1010 steel substrates in: (a) 0.1 M Pb(NO₃)₂ + 2.0 M NaOH + 0.2 M sorbitol at various RDE rotation speeds (ω /Hz): (—) 0.0; (···) 0.25, (---) 0.5; (- - -) 0.75, (- · - ·) 1.0; (- - - -) 1.25; (- - - - -) 1.5 at 10 mV s⁻¹; (b) variation of J_L with $\omega^{1/2}$ for lead electrodeposition on to steel RDE.

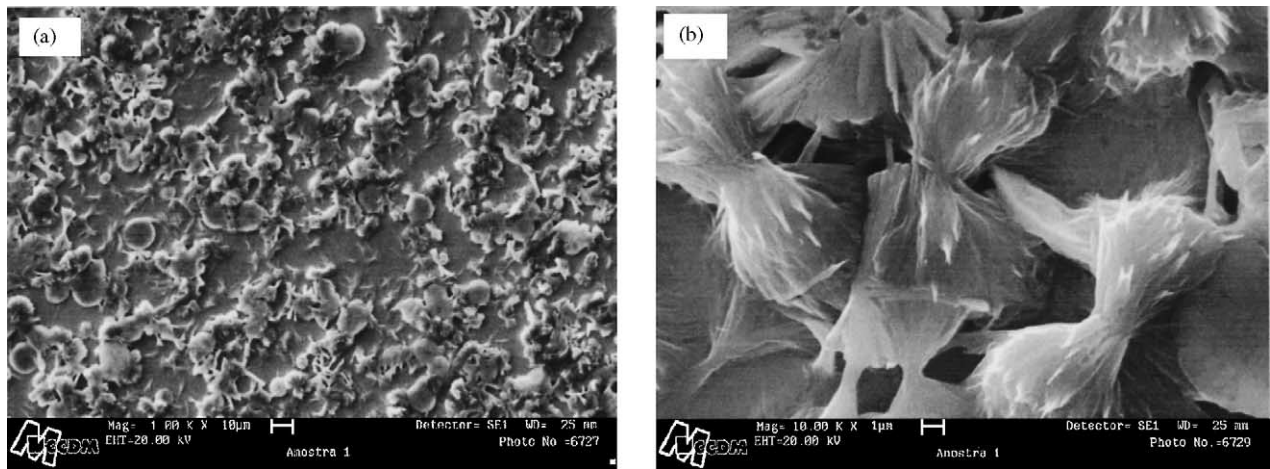


Fig. 7. SEM micrographs for lead films obtained in potential sweeps from -0.45 to -0.86 V; at low (a) and high (b) magnifications. Electrolytic solution: 0.1 M Pb(NO₃)₂ + 2.0 M NaOH + 0.2 M sorbitol.

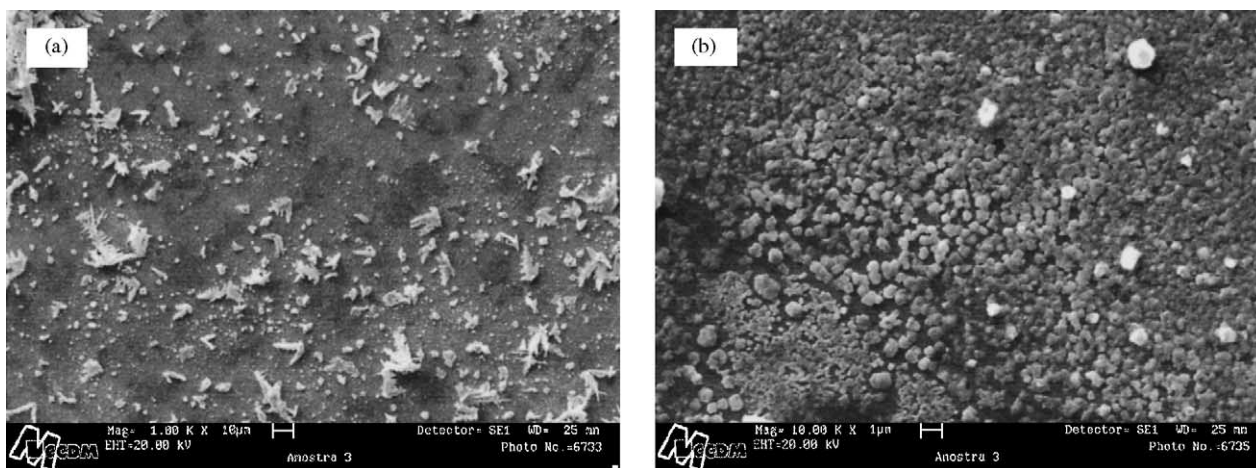


Fig. 8. SEM micrographs for lead films obtained in potential sweeps from -0.45 to -1.0 V; at low (a) and high (b) magnifications. Electrolytic solution: 0.1 M $\text{Pb}(\text{NO}_3)_2$ + 2.0 M NaOH + 0.2 M glycerol.

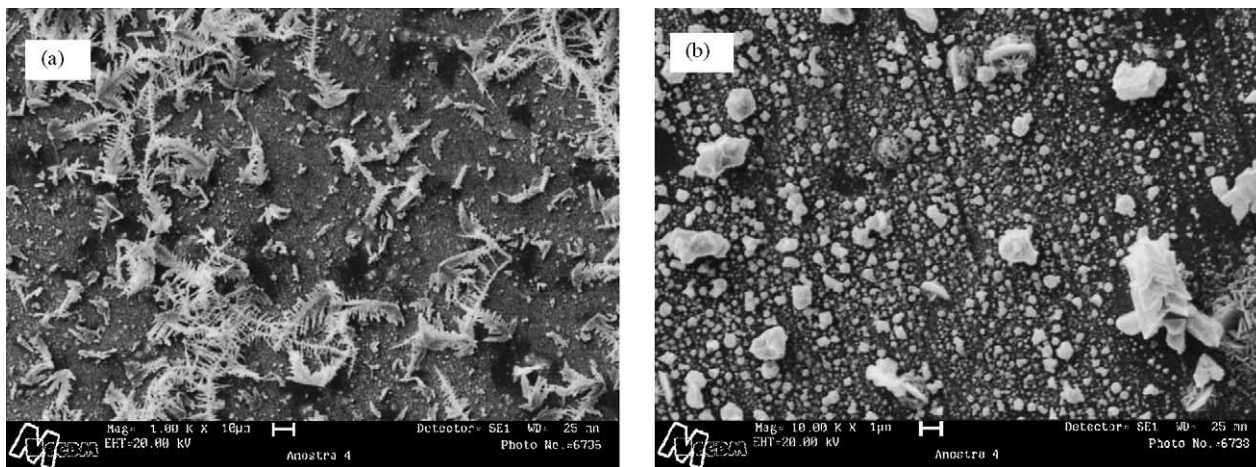


Fig. 9. SEM micrographs of Pb films obtained in potential sweeps from -0.45 to -1.5 V; at low (a) and high (b) magnifications. Electrolytic solution: 0.1 M $\text{Pb}(\text{NO}_3)_2$ + 2.0 M NaOH + 0.2 M sorbitol.

4. Conclusions

Potentiodynamic curves indicated that in the first moments of the lead deposition process, it is characterized by high change current density, but that beyond the peak potential it is controlled by mass transport, leading to production of non-adherent lead film. The value of the rate-limiting diffusion coefficient was $4.0 \times 10^{-6} \text{ cm}^2 \text{ s}^{-1}$. The undercutting of lead film at the top of the anodic peak allowed a pure lead powder to be collected. The presence of sorbitol as an additive in the plating bath modified the current density of the cathodic process more significantly than did the presence of glycerol in the plating bath. From the SEM results, it can be inferred that sorbitol has a beneficial effect on the lead deposition, since it reduces the propagation of dendritic growth more than glycerol, corroborating the decrease in

the deposition current density in the presence of this additive.

Acknowledgements

Financial support from Brazilian agencies FAPESP (Proc. No. 10145-4/98) and CNPq is gratefully acknowledged.

References

- [1] R. Calusaru, *Electrodeposition of Metal Powders*, Elsevier, Amsterdam, 1979.
- [2] N.V. Parthasaday, *Practical Electroplating Handbook*, Prentice-Hall, Englewood Cliffs, NJ, 1989.
- [3] D. Pletcher, *Industrial Electroplating*, Chapman & Hall, New York, 1982.

- [4] F.A. Lowenheim, *Modern Electroplating*, 2nd Edition, Wiley, New York, 1974.
- [5] A.G. Morachevskii, *Russian J. Appl. Chem.* 70 (1) (1997) 1–12.
- [6] C. Weiping, T. Yizhuang, B. Kejun, Z. Yue, *Trans. Nonferrous Met. Soc. China* 6 (4) (1996) 47.
- [7] C. Weiping, C. Fancai, P. Yanbing, L. Qizhong, B. Kejun, Z. Yue, *Trans. Nonferrous Met. Soc. China* 7 (3) (1997) 155.
- [8] A.G. Morachevskii, A.I. Demidov, Z.I. Vaisgant, M.S. Kogan, *Russian J. Appl. Chem.* 69 (3) (1996) 412–414.
- [9] I.A. Carlos, M.A. Malaquias, M.M. Oizume, T.T. Matsuo, *J. Power Sources* 92 (2001) 56–64.
- [10] I.A. Carlos, C.A.C. Souza, E.M.J.A. Pallone, R.H.P. Francisco, V. Cardoso, B.S. Lima-Neto, *J. Appl. Electrochem.* 30 (2000) 987.
- [11] A. Molenaar, J.W.G. de Bakker, *J. Electrochem. Soc.* 136 (2) (1989) 378–382.
- [12] M.R.H. de Almeida, I.A. Carlos, L.L. Barbosa, R.M. Carlos, B.S. Lima-Neto, E.M.J.A. Pallone, *J. Appl. Electrochem.* 32 (2002) 763–773.
- [13] L.L. Barbosa, Ph.D. thesis, Universidade Federal de São Carlos, Brazil, 2001.
- [14] S. Fletcher, *Electrochim. Acta* 28 (7) (1983) 917–923.
- [15] B.J. Allen, L. Faulkner, *Electrochemical Methods, Fundamentals and Applications*, Wiley, New York, 1980.
- [16] S.E. Group, *Instrumental methods in electrochemistry*, in: T.J. Kemp (Ed.), *Ellis Horwood Series in Physical Chemistry*, Wiley, New York, 1985.
- [17] I.M. Kolthoff, J.J. Lingane, *Polarography*, vol. 1, Interscience, New York, 1952.